Towards the neuroarchitectural underpinning of brain functions and functional recovery after acute ischemic stroke - A rich-club organization perspective

Abstract

Stroke is one of the major diseases that causes disabilities, such as motor impairment. The ability of the brain to reorganize underlies functional recovery. Studies have shown that rich-club, highly connected and central brain regions, may underlie brain function and be associated with many brain disorders. In this study, we aimed to comprehensively analyse the relation between motor functions and rich-club organization of the brain network of patient after first-time acute ischemic stroke, and to investigate the biomarkers that may help predict poststroke functional recovery. A cohort of 16 first-time acute ischemic stroke patients was recruited. Structural brain networks were measured using diffusion tensor imaging and T2-weighted imaging within 1 week and at 1, 3 and 6 months after stroke. Motor functions were assessed using the Upper-Extremity Fugl-Meyer motor scale and Barthel Index at the same time points. Most of the rich-club regions were stable over the course of stroke recovery. The left supplementary motor area, left anterior cingulate gyrus, right putamen, and left insula became rich-club region at one point in time after stroke. The network properties of a number of brain regions, majority being non-rich-club regions, changed with time after stroke. Of all the metrics of brain network at rich-club scale that correlate with recovery, the communication cost of rich-club connections, communication cost ratio of feeder connections, density of local connections and normalized rich-club coefficient were found to be prognostic indicators of poststroke functional recovery.

Introduction

Approximately 80% of patients suffer from motor impairment after stroke.[1,2] Brain plasticity mechanisms, including activity-dependent rewiring and synapse strengthening, may likely underlie the recovery of brain functions.[3–6] Previous studies have investigated the relation between motor recovery after stroke and the structural connectivity of local pathways, such as corticospinal[7–10], alternate corticofugal[11,12] and corticocortical pathways[13–15]. The relation between motor recovery and structural connectivity in stroke patients has also been investigated by large-scale analysis of structural connectivity[16].

Neuroarchitecture can be understood not only at the local and global scales, as is usually performed, but also in specific groups of brain regions and the relationship among them, known as rich-club organization[17,18]. Rich-club organization is composed of brain regions that are closely connected, i.e., high centrality, and has been found to serve brain functions[19]. Rich-club organization may dominate the entire brain network[17], and has been regarded as the core of communication of the whole human brain[20,21]. The brain regions that form rich-club organization in healthy adults are bilateral frontoparietal and subcortical regions, including the precuneus, superior frontal cortex, parietal cortex, putamen, hippocampus and thalamus.[22] Neurological diseases and disorders, such as, schizophrenia[23], Huntington's disease[24], multiple sclerosis[25], traumatic brain injury[26], and Alzheimer's disease[27], have been shown to impair rich-club organization.

Two prior studies have investigated the relation between poststroke functional outcomes related to motor function and rich-club metrics, such as the number of rich-club nodes affected by stroke[28] and path length[29]. Considering that there is a lack of understanding of the longitudinal changes in rich-club organization after stroke and the relation between motor functional outcomes and rich-club organization, we therefore aimed to investigate whether rich-club organization would change over the course of stroke recovery and to investigate the network metrics that may predict motor recovery.

Materials and methods

Subjects and functional assessments

Stroke patients (n = 16; 11 male; mean age 65.8 ± 11.0; infarct side: 50% left) with first-time acute ischemic stroke were recruited between September 2015 and July 2018 with informed consent. MRI and functional assessments were performed within 1 week (n = 12) and at 1 (n = 16), 3 (n = 13) and 6 (n = 9) months after acute ischemic stroke. Functional assessments

included the Upper-Extremity Fugl-Meyer motor scale (UE-FM) and Barthel index (BI). The UE-FM was developed to quantitatively assess the severity of motor impairment of the upper extremity due to hemiplegic stroke and is based on the well-defined stages of motor recovery[30]. The BI was developed to quantitatively assess disability and functional outcomes[31]. All patients received rehabilitation at the Acute Stroke Unit of Queen Mary Hospital after admission due to acute stroke. After an average of 5 days after admission, patients were transferred to the Stroke Rehabilitation Ward of Tung Wah Hospital for more intensive rehabilitation. All patients underwent conventional occupational rehabilitation therapy sessions, including activities of daily living training, upper limb functional training, cognitive perceptual training and functional task training. All procedures were carried out following the operational guidelines of the Human Research Ethics Committee, and all protocols were approved by the Institutional Review Board of the University of Hong Kong/Hospital Authority Hong Kong West Cluster.

Image acquisition

All MRI scans were performed using a 3.0 T MRI scanner (Achieva TX, Philips Healthcare, Best, The Netherlands) with a body coil for excitation and an 8-channel head coil for reception. Diffusion tensor imaging (DTI) was performed using single-shot spin-echo echo planar imaging, consisting of non-diffusion-weighted images (b0) and diffusion-weighted images (DWIs) with b-values of 1000 s/mm^2 along 32 gradient directions, with the following parameters: TR/TE = 4000/81 ms, field-of-view = 230 × 230 mm^2, reconstructed resolution = 3 × 3 mm^2, 33 contiguous slices with thickness of 3 mm, SENSE factor = 2, number of averaging = 2, total scan time ≈ 5 minutes. TI-weighted image were acquired using 3D magnetization prepared-rapid gradient echo (MPRAGE) with the following parameters: TR/TE/TI = 7/3.17/800 ms, field-of-view = 240 × 240 mm^2, reconstruction resolution = 1 × 1 × 1 mm^3, 160 contiguous slices, scan time ≈ 6 min.

Image pre-processing

All of the pre-processing procedures were performed using SPM12 (https://www.fil.ion.ucl.ac.uk/spm/). Head motion correction was performed by registering DWIs to b0 images[32]. MPRAGE images were first reoriented taking the anterior commissure[33] as the origin. The reoriented MPRAGE images were normalized to the MNI152 template to obtain a transformation matrix M. The MNI152 template was then inversely normalized to MPRAGE images by the inverse of M, M^{-1}. The inverse normalized MNI152 template was

non-linearly registered to DWIs, and a transformation matrix T was obtained. In this way, an inverse warping transformation from the standard space to the native DTI space was obtained.

Network construction

Tractography: Diffusion tensor and diffusion metrics were obtained using the Diffusion Toolkit[32]. White matter tractography was obtained using TrackVis (http://trackvis.org) using Fibre Assignment by Continuous Tracking (FACT)[35,36] with an angle threshold of 45° and random seed of 32. Spine filter was used to smooth the fibre tracks.

Network node definition: The Automated Anatomical Labelling 2 (AAL2) atlas[37] in the standard space was inversely wrapped to the individual DTI native space according to M^{-1} and T. Ninety-four cortical regions (47 in each hemisphere) were obtained, and each region was regarded as a node. Of these, 8 regions were excluded, namely, the left and right inferior occipital gyrus, left and right superior temporal pole, left and right middle temporal pole and left and right inferior temporal pole, due to variations in brain coverage.

Network link definition: The UCLA Multimodal Connectivity package was used to calculate the number and length of fibres between each pair of regions. Two regions were considered as connected when a fibre connected them. The link weight was defined as the fibre count between two regions.

Network topology metrics

MATLAB (2018b) and the Brain Connectivity Toolbox (https://sites.google.com/site/bctnet/) were used to calculate brain network topology metrics. The metrics included (1) node degree, the number of nodes that a given node is connected to; (2) node strength, the sum of the weight of connected links of a node; (3) local clustering coefficient, the connection properties within the neighbourhood of a node; (4) global efficiency, the average inverse shortest path length in the network; (5) local efficiency, the global efficiency computed on node neighbourhoods; and (6) node betweenness centrality, the fraction of all shortest paths in the network that contain the node of interest.

Rich-club organization

R (3.6.0) was used to estimate rich-club organization for each subject at each time point using a previously published method[16]. The weighted rich-club coefficient was calculated in 4 steps. First, for each node degree (k), a subnetwork was obtained by extracting the nodes with degree

greater than k and the links among them. Second, for each subnetwork, the total number of links (n) and the sum of weights of the links (W) were calculated. Third, the n largest weights of the whole network were summed. Finally, the weighted rich-club coefficient of this subnetwork was subsequently calculated as follows:[38]

$$\varphi^{w}(\mathrm{k}) = \frac{W_{>k}}{\sum_{l=1}^{n} w_l^{ranked}},$$

where $W_{>k}$ represents total weights of the links of nodes with degree larger than k, and $\sum_{l=1}^{n} w_l^{ranked}$ the sum of the n largest weights of the links. However, nodes with lower degree in a network have lower possibilities of sharing links with each other by coincidence, and even random networks generate increasing rich-club coefficients as a function of increasing degree threshold k. To circumvent this effect, 1,000 random networks with the same size and same degree distribution of the network of interest were generated. The average of the rich-club coefficients of the 1,000 random networks were calculated, φ_{random}. The normalized rich-club coefficient of the network of interest was defined as follows:[17,18]

$$\varphi_{norm} = \frac{\varphi_k}{\varphi_{random}}$$

A subnetwork is considered a rich-club organization when $\varphi_{norm}(k) > 1$[39,40].

A node can be evaluated as a rich-club node when k ={k_1, k_2, …, k_n}, in which the highest k was called the highest rich-club level. Each node of a rich-club organization was given a score according to their highest rich-club level Then, after averaging the score of nodes from all participants at the same time point after stroke, the top 8 nodes (i.e., 10% of all nodes) were selected as rich-club nodes.

Node and connection types

There are two types of nodes in a brain network, namely, rich-club nodes and peripheral nodes. Furthermore, there are three types of connections in a rich-club organization, namely, rich-club connections (between rich-club nodes), feeder connections (between rich-club nodes and non–rich-club nodes), and local connections (between non–rich-club nodes).[41]

Network communication

The cost of a link was defined as the product between its length and density (the count of streamlines between two brain regions). Communication cost was defined as the product between length and density based on their topological distance[41]. To calculate the

communication cost of the three kinds of connections in a rich-club organization, first, the shortest paths between 84 nodes were calculated. Then, each link of the shortest paths was divided into three categories (rich-club, feeder and local connections). Next, the communication cost of each link was calculated by multiplying its length and density. Finally, the communication cost of three kinds of connections was obtained by summing the communication cost for links of each kind. The metric ratio of a connection type was defined as the sum of metrics of this connection type divided by the total metric of the whole network. For example, density ratio of rich club connections was defined as total density of rich club connections divided by total density of all connections. The communication cost/density ratio was defined as the communication cost ratio divided by the density ratio, which was the weight of brain communication capacity[41].

Statistical analysis

Statistical analyses were performed by R (version 3.6.0) with the functions lmer (https://cran.r-project.org/web/packages/lme4/lme4.pdf) and blmer (https://cran.rproject.org/web/packages/blme/blme.pdf). To simplify the statistical analyses on the local structural brain networks, the left and right hemispheres were flipped so that the left hemisphere always corresponded to the ipsilesional hemisphere. Due to attrition, some of the behavioural data and imaging data were not obtained. Imputation was thus performed on the behavioural data to increase the effective sample size for subsequent statistical analyses of prediction model. For patients no. 2, 13 and 15, the behavioural data at 6 months after stroke were imputed from those at 3 months. Since patient nos. 11 and 16 had already made full recovery at the last follow-up, full behavioural scores were assumed for the missing time points. After imputation, the 10 patients had behavioural data for all 4 time points. The imputed behavioural data are underlined in Table 1.

To handle data with an unequal number of longitudinal measures, a Bayesian linear mixed model[42,43] was used as the main model in the current study so that a posteriori estimation could be maximized in a Bayesian setting. When necessary, linear mixed models were followed by post hoc tests with Bonferroni corrections for multiple comparisons at $p < 0.05$. This study mainly investigated three aspects: (1) to test whether functional assessments and network metrics changed with time. Models were established with the functional assessments and network metrics as responses, time as fixed variable, each subject as random variable, and age and gender as covariates. (2) To test the correlations between network metrics and functional assessments, models were established with the functional assessment data as responses,

network metrics as fixed variables, each subject as random variable, and age and gender as covariates. (3) To identify biomarkers that may predict poststroke functional recovery, models were established with poststroke functional recovery (change in functional assessment from baseline) as responses, each subject as random variable, metrics at baseline as fixed variables, and time, age and gender as covariates. After selecting the metrics that may be predictors of responses, a linear mixed regression model was established by the stepwise method. In the whole study, a best fitting model was chosen by comparing models using the likelihood ratio test with the principle that the smaller the AIC was, the better the model was[44]. Additionally, the simpler model was chosen when the gap in AIC values and likelihood ratio test results was small.

Table 1. The baseline demographics and assessment of motor impairment (Upper-Extremity Fugl-Meyer motor scale) and performance in activities of daily living (Barthel Index) of n = 16 patients.

Patient	Age	Sex	Handedness	Side of lesion	Upper-Extremity Fugl-Meyer Motor Scale (0–66)				Barthel Index (0–100)			
					< 1 week	1 month	3 months	6 months	< 1 week	1 month	3 months	6 months
1	63	F	R	R	33	64	66	66	55	90	100	100
2	44	M	R	L	N.A.	63	63	63	N.A.	95	100	100
3	50	M	R	L	N.A.	5	14	18	N.A.	65	85	100
4	63	M	R	R	0	2	N.A.	N.A.	0	40	N.A.	N.A.
5	70	M	R	L	N.A.	31	40	49	N.A.	65	80	85
6	74	M	R	R	N.A.	48	62	63	N.A.	25	75	95
7	65	M	R	L	0	7	13	20	35	40	45	70
8	84	F	R	R	0	5	5	5	30	50	50	50
9	63	M	R	L	56	64	66	66	55	60	100	100
10	61	M	R	L	54	59	64	64	55	85	95	100
11	71	F	R	R	60	66	66	66	65	100	100	100
12	57	M	R	L	0	3	30	45	45	30	75	90
13	84	M	R	L	0	60	66	66	0	70	95	95
14	79	F	R	R	2	33	N.A.	N.A.	30	40	N.A.	N.A.
15	63	M	R	R	0	4	4	4	0	50	60	60
16	62	F	R	R	64	66	66	66	80	100	100	100

R: right; L: left; N.A.: not available

Note that functional assessments that were underlined were obtained from data imputation.

Results

Patient demographics

MRI and functional assessments were performed on 12, 16, 13 and 9 patients within 1 week and at 1, 3 and 6 months after first-time acute ischemic stroke, respectively, as shown in **Table 1**. A linear mixed model was used to test the fixed effect of time on functional assessments. UE-FM ($\beta_{time} = 3.47$; $\chi_1^2 = 13.68$, p < 0.001; **Figure 1A**) and BI ($\beta_{time} = 7.94, \chi_1^2 = 28.31$, p < 0.001; **Figure 1B**) significantly increased with time. Post hoc tests showed that UE-FM scores at 1 (p = 0.01), 3 (p < 0.001) and 6 (p < 0.001) months were significantly higher than those within 1 week after stroke. BI scores at 1, 3 and 6 (p < 0.001, all) months were significantly higher than those within 1 week after stroke, and BI scores at 3 and 6 (p < 0.001, all) months were significantly higher than 1 month after stroke.

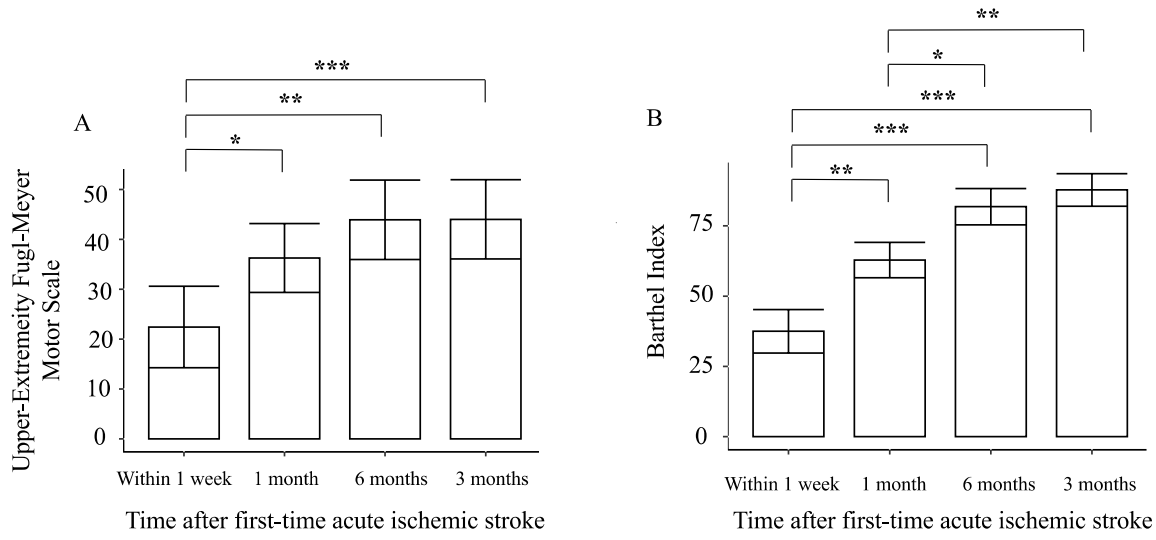

Figure 1. Bar chart with error bars (standard deviations) of the (A) Upper-Extremity Fugl-Meyer motor scale and (B) Barthel index scores within 1 week (n = 12), and at 1 (n = 16), 3 (n = 13) and 6 (n = 9) months after first-time acute ischemic stroke. Post hoc tests with Bonferroni corrections for multiple comparisons across different time points were performed (*p <0.05, **p<0.01, ***p<0.001).

Rich-club organizational changes after stroke

Rich-club organization was found from the structural brain network of patients within 1 week (**Figure 2 A**), and at 1 (**Figure 2 B**), 3 (**Figure 2 C**) and 6 months (**Figure 2 D**) after first-time acute ischemic stroke. Not every patient (grey lines) had a normalized rich-club coefficient larger than 1 except at 6 months after stroke. The brain regions that were rich-club regions at the 4 time points after stroke were listed in **Table 2**. The rich-club regions within 1 week after stroke were the left and right dorsolateral superior frontal gyri, left and right supplementary motor areas, right insula, right anterior cingulate and paracingulate gyri, left and right median

cingulate and paracingulate gyri. At 1 month, left anterior cingulate and paracingulate gyri became a rich-club region, and left supplementary motor area became a peripheral region. At 3 months, right putamen became a rich-club region, and the left anterior cingulate reverted to a peripheral region. At 6 months, left insular became a rich-club region, and the right putamen reverted to a peripheral region.

Table 2 Rich-club regions at 4 time points after first-time acute ischemic stroke.

Rich-club regions	Side*	Time after acute ischemic stroke			
		< 1 week	1 month	3 months	6 months
Dorsolateral superior frontal gyrus	Left	√	√	√	√
	Right	√	√	√	√
Supplementary motor area	Left	√			
	Right	√	√	√	√
Insular	Left				√
	Right	√	√	√	√
Median cingulate and paracingulate gyri	Left	√	√	√	√
	Right	√	√	√	√
Anterior cingulate and paracingulate gyri	Left		√		
	Right	√	√	√	√
Putamen	Right			√	

*Left hemisphere was assigned as the ipsilesional hemisphere and right contralesional hemisphere.

Linear mixed model was used to test the effect of time after stroke on normalized rich-club coefficient for $0 < k < 34$. Significant time effect on the normalized rich-club coefficients were observed for $20 \leq k \leq 23$, k = 20 ($\chi_1^2 = 7.22$, p = 0.007, $\beta_{time} = 0.01$), 21 ($\chi_1^2 = 6.87$, p = 0.008, $\beta_{time} = 0.01$), k = 22 ($\chi_1^2 = 6.83$, p = 0.008, $\beta_{time} = 0.01$), and k = 23 ($\chi_1^2 = 6.30$, p = 0.012, $\beta_{time} = 0.01$).

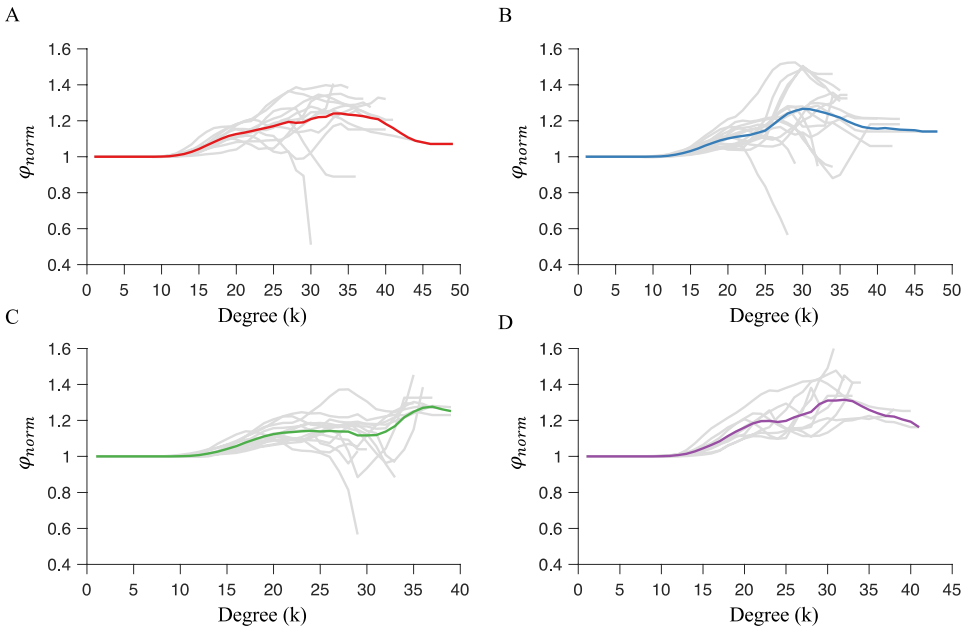

Figure 2. Normalized rich-club coefficient of the structural brain network of patient within (A) 1 week and at (B) 1, (C) 3 and (D) 6 months after first-time acute ischemic stroke. Grey lines: individual patient; Colored lines: average of all patients.

Longitudinal changes in network metrics after first-time acute ischemic stroke

The structural brain network over the course of stroke recovery were examined at nodal and rich-club scale. Metrics of the network at nodal scale pertain to the network metrics of each brain region; rich-club scale to the mean link metrics of rich-club, feeder and local connections;

A linear mixed model was used to test the fixed effect of time after stroke on the metrics of brain network at nodal (**Figure 3**) and rich-club (**Table 3**) scales with age and gender as covariates, and subject as random variable. For local scale, the node degree (**Figure 3A**), node strength (**Figure 3B**), local clustering coefficient (**Figure 3C**), local efficiency (**Figure 3D**), and nodal betweenness centrality (**Figure 3E**) of a number of nodes changed with time after stroke. For rich-club scales, the significant negative time effect on density ($\beta_{time} = -8.93, \chi_1^2 = 4.57,\ p = 0.33$) and density ratio ($\beta_{time} = -0.01, \chi_1^2 = 4.74, p = 0.029$) of local connections were observed. Significant positive time effect on the density ratio of feeder connections ($\beta_{time} = 0.01, \chi_1^2 = 7.06, p = 0.008$), and communication cost ratio ($\beta_{time} = 0.01, \chi_1^2 = 5.43, p = 0.020$) and communication cost ratio/density ratio ($\beta_{time} = 0.14, \chi_1^2 = 5.15, p = 0.023$) of rich-club connections were also observed.

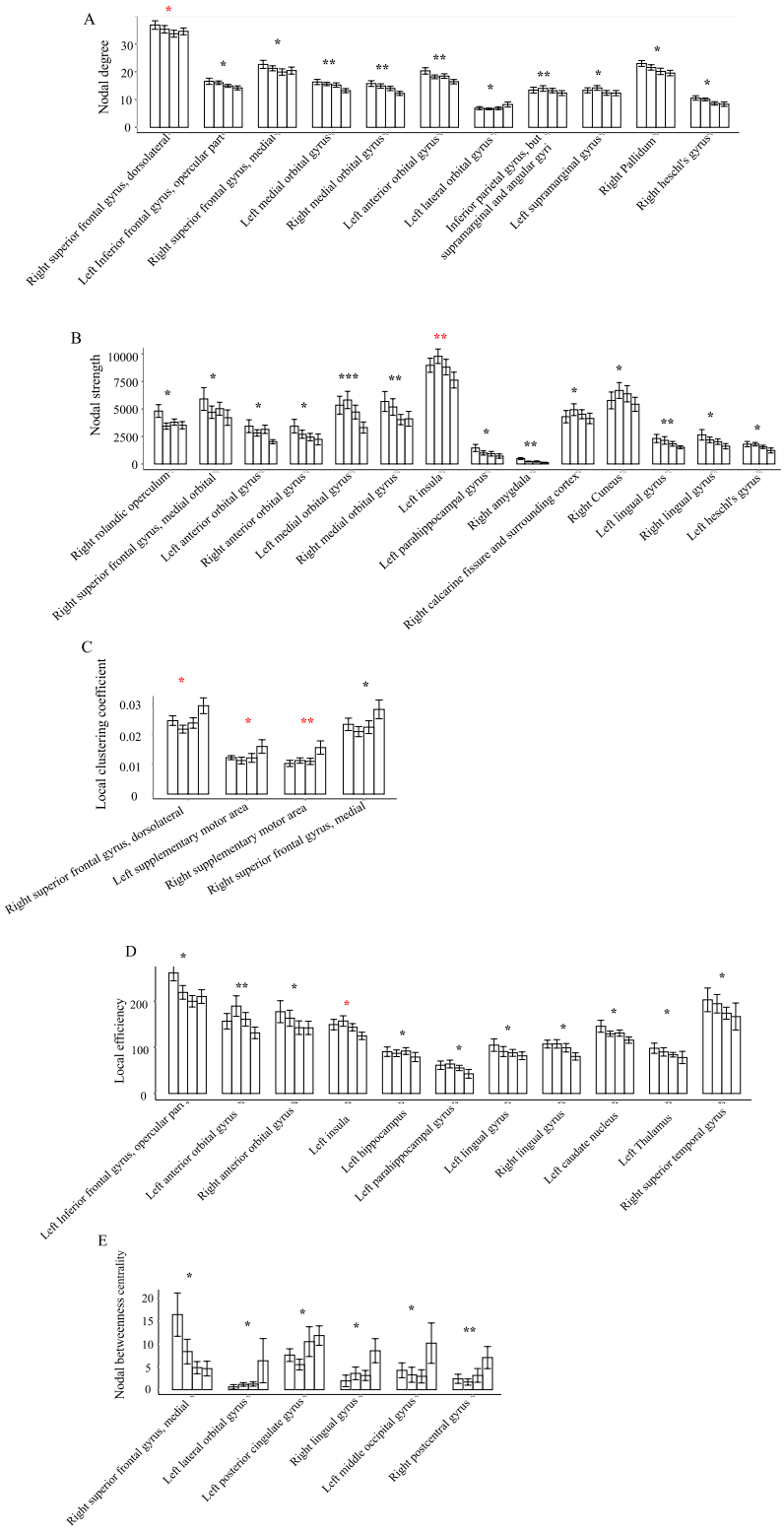

Figure 3. The effect of time after first-time acute ischemic stroke on the metrics of brain network at local scale: (A) node degree, (B) node strength, (C) local clustering coefficient, (D) local efficiency and (E) nodal betweenness centrality. Only regions showing statistical significance were displayed. *****p<0.05, ******p<0.01, *******p<0.001. Rich-club regions were annotated with a red *****.

Table 3. The effect of time after first-time acute ischemic stroke on the metrics of brain network at rich-club scales. Only metrics showing statistical significance were shown.

Node/Connection Type	Network metric	β_0	β_1	χ^2	Df	Pr (> χ^2)
Rich-club connections	Communication cost ratio	0.02	0.01	5.43	1	0.020
	Communication cos ratio/density ratio	0.13	0.14	5.15	1	0.023
Feeder connections	Density ratio	0.29	0.01	7.06	1	0.008
Local connections	Density	281.80	-8.93	4.57	1	0.033
	Density ratio	0.66	-0.01	4.74	1	0.029

β_0 and β_1 are the fixed effects coefficients: β_0 is the intercept, β_1 is the linear slope; Df: degrees of freedom for the chi-square test. UE-FM: upper-extremity Fugl-Meyer motor scale; BI: Barthel index.

Relation between functional assessment and network metrics

A linear mixed model was used to test the relation between the metrics at rich club scale of brain network and functional assessment with age and gender as covariates, and subject as random variable. The communication cost ratio ($\beta_1 = -72.81, \chi_1^2 = 5.62, p = 0.018$) and communication cost ratio/density ratio ($\beta_1 = -41.21, \chi_1^2 = 4.66, p = 0.031$) of local connections were correlated with UE-FM. The communication cost ratio ($\beta_1 = -133.30, \chi_1^2 = 7.86, p = 0.005$) and communication cost ratio/density ratio ($\beta_1 = -64.11, \chi_1^2 = 4.34,\ p = 0.037$) of local connections, and mean length of feeder ($\beta_1 = -0.35, \chi_1^2 = 4.48, p = 0.034$) and local connections ($\beta_1 = -0.20,\ \chi_1^2 = 5.84, p = 0.016$) were correlated with BI. All statistical results were summarized in **Table 4**.

Table 4. Correlation between functional assessments versus rich club metrics.

Functional assessment	Node/Connection type	Network metric	β_0	β_1	χ^2	Df	Pr (> χ^2)
UE-FM	Local connections	Communication cost ratio	89.09	-72.81	5.62	1	0.018
		Communication cost ratio/density ratio	87.83	-41.21	4.66	1	0.031
BI	Feeder connections	Mean length	180.50	-0.35	4.48	1	0.034
	Local connections	Mean length	177.10	-0.20	5.84	1	0.016
		Communication cost ratio	174.65	-133.30	7.86	1	0.005
		Communication cost ratio/density ratio	170.42	-64.11	4.34	1	0.037

β_0 and β_1 are the fixed effects coefficients: β_0 is the intercept, β_1 is the linear slope; Df: degrees of freedom for the chi-square test. UE-FM: upper-extremity Fugl-Meyer motor scale; BI: Barthel index.

scale

The metrics of brain network at rich-club scale that were included in subsequent linear mixed model were selected by comparing the model with and without the network metric with each subject as random variable, network metric to be tested as fixed variable, and time, age and gender as covariates. Linear mixed models were subsequently used to investigate the relation between changes in functional assessments from baseline (i.e., poststroke functional recovery) and metrics of brain network at rich-club scale as well as normalized rich club coefficient at the first time point. The communication cost of rich-club ($\beta = -0.01, \chi_1^2 = 10.06, p = 0.002$), normalized rich-club coefficients (k = 20)($\beta = 197.16, \chi_1^2 = 4.29, p = 0.038$), density ($\beta = -0.13, \chi_1^2 = 3.89, p = 0.049$) length ($\beta = -0.18, \chi_1^2 = 6.29, p = 0.012$), cost ($\beta = -0.13, \chi_1^2 = 7.63, p = 0.006$), communication cost ($\beta = -0.002, \chi_1^2 = 6.46, p = 0.011$), communication cost ratio ($\beta = -264.24, \chi_1^2 = 4.86, p = 0.028$) of local connections, and cost ($\beta = -0.24, \chi_1^2 = 7.44, p = 0.006$), communication cost ($\beta = -0.002, \chi_1^2 = 10.03, p = 0.002$) and communication cost ratio ($\beta = -367.92, \chi_1^2 = 5.06, p = 0.024$) of feeder connections were correlated with the change in UE-FM. The density of local connections ($\beta = -0.14, \chi_1^2 = 4.65, p = 0.031$), communication cost ratio of feeder ($\beta = 455.67, \chi_1^2 = 7.85, p = 0.005$) and local ($\beta = -306.06, \chi_1^2 = 6.24, p = 0.012$) connections, and normalized rich-club coefficients were correlated with the changes in BI. These results were summarized in **Table 5**.

The network metrics that were selected to predict poststroke functional recovery were shown in **Table 6**. The communication cost of rich-club connections，communication cost ratio of feeder connections and normalized rich-club coefficients (k = 20) could predict UE-FM changes ($\chi_1^2 = 17.96$, p < 0.001). The density of local connections, communication cost ratio of feeder connections and rich-club coefficients (k =18, 19, 20) could predict BI changes ($\chi_1^2 = 26.16$, p < 0.001)

Table 5. Correlation between poststroke functional recovery versus metrics of brain network at rich-club scales.

Poststroke functional recovery*	**Node/Connection type**	**Metric**	**β_0**	**β_1**	**χ^2**	**Df**	**Pr (> χ^2)**
Change in UE-FM	Local connections	Density	-76.38	-0.13	3.89	1	0.049
		Length	-55.90	-0.18	6.29	1	0.012
		Cost	-83.26	-0.13	7.63	1	0.006
		Communication cost	-76.97	-0.002	6.46	1	0.011
		Communication cost ratio	-32.37	-264.24	4.86	1	0.028
	Feeder connections	Cost	-54.98	-0.24	7.44	1	0.006
		Communication cost	-60.98	-0.002	10.03	1	0.002
		Communication cost ratio	-267.46	367.92	5.06	1	0.024
	Rich-club	Communication cost	-59.61	-0.01	10.06	1	0.002
		$\emptyset_{norm}$ (k = 20)	-311.17	197.16	4.29	1	0.038
Change in BI	Local connections	Density	-66.32	-0.14	4.65	1	0.031
		Communication cost ratio	59.43	-306.06	6.24	1	0.012
	Feeder connections	Communication cost ratio	-304.27	455.67	7.85	1	0.005
	Rich-club	$\emptyset_{norm}$ (k = 17)	-335.69	240.51	4.36	1	0.037
		$\emptyset_{norm}$ (k = 18)	-434.11	314.70	7.95	1	0.005
		$\emptyset_{norm}$ (k = 19)	-507.54	365.69	16.21	1	< 0.001
		$\emptyset_{norm}$ (k = 20)	-485.59	347.95	16.90	1	< 0.001
		$\emptyset_{norm}$ (k = 21)	-378.11	260.42	6.93	1	0.008
		$\emptyset_{norm}$ (k = 22)	-339.23	229.89	7.92	1	0.005

β_0 and β_1 are the fixed effects coefficients: β_0 is the intercept, β_1 is the linear slope; Df: degrees of freedom for the chi-square test. UE-FM: upper-extremity Fugl-Meyer motor scale; BI: Barthel index. $\emptyset_{norm}$: normalized rich club coefficient; k: degree; index.

*Poststroke functional recovery was defined as the changes in functional assessments from baseline.

Table 6. Summary of prediction models.

Response	Model	Variables	AIC	BIC	χ^2	Df	Pr (> χ^2)
Change in UE-F	Baseline	Age, gender, time	253.33	262.13			
	Prediction	Age, gender, time, communication cost of rich club connections, communication cost ratio of feeder connections, $\emptyset_{norm}$ (k = 20)	241.38	254.57	17.96	3	< 0.001
Change in BI	Baseline	Age, gender, time	278.35	287.15			
	Prediction	Age, gender, time, density of local connections, communication cost ratio of feeder connections, $\emptyset_{norm}$ (k = 18, 19, 20)	262.19	278.32	26.16	5	< 0.001

AIC: Akaike information criterion; BIC: Bayesian information criterion. Df: degrees of freedom for the chi-square test. UE-FM: upper-extremity Fugl-Meyer motor scale; BI: Barthel index. $\emptyset_{norm}$: normalized rich club coefficient; k: degree; index.

Discussion

Our study aims to comprehensively analyse the relation between functional assessments (i.e., UE-FM and BI scores) and rich-club organization of the brain network of patient after first-time acute ischemic stroke. First of all, we investigated the effect of time after stroke on functional assessments, rich club organization and metrics of the brain network at rich club and local scales. Second, we examined the relation between functional assessment versus rich club organization and network metrics. Finally, we established models to predict poststroke functional recovery (change in functional assessment from baseline) using metrics of brain network at rich-club scale and normalized rich club coefficient.

Longitudinal changes in brain network after stroke

87.5% of the rich-club regions were stable over the course of stroke recovery, including the bilateral dorsolateral superior frontal gyrus, right supplementary motor area, right insula, right anterior cingulate gyrus, and bilateral median cingulate gyri. The brain regions that became rich-club at one point in time after stroke included the left supplementary motor area, left anterior cingulate gyrus, right putamen, and left insula, which appeared at the last time point. These results suggest that stroke recovery may require remodelling of rich-club organization largely in the ipsilesional hemisphere, and that minority of the rich-club regions changed

throughout the course of stroke recovery, supporting the notion that rich-club organization may likely be the backbone of brain communication[19,20,46] so that a little change in rich club organization may affect brain function. Despite the fact that patients have functionally recovered at 6 months after stroke, their rich club regions were not the same as those in the study by van den Heuvel et al [45]. This discrepancy may be due to the fact that the brain network of these patients may conceivably be different from healthy controls, or difference in postprocessing of brain network, such as the thresholds for determining whether two regions were connected.

Nodal analysis and network metrics at rich club scale analysis were performed to investigate the detailed longitudinal changes in brain network. The network properties of a number of brain regions, majority of which were not rich-club regions, changed with time after stroke except local clustering coefficient, a metric present how closely other nodes connect with itself. Among four regions changed in clustering coefficients, three of them were rich-club regions, including the right dorsolateral superior frontal gyrus and left and right supplementary motor areas, indicating the importance of connections closeness of rich club regions in the course of stroke recovery. No rich-club regions were found to change in betweenness centrality, and only one among the rich-club regions changed in degree, showing difference from findings of patients with Huntington's disease[48] , in which the degree of the rich-club regions showed dramatic changes. Among rich club regions, only left Insular was found to change in both strength and local efficiency. A possible explanation is that the insula is an integral brain hub connecting functional systems including motor control as previous reported. Communication cost ratio and communication cost ratio/density ratio of rich-club connections were positively affected by time indicates communication of rich club would be more active and larger capacity of communication as time went by so that can serve more communication task under its physical structure. Mean density and Density ratio of local connections were negatively affected by time and density ratio of feeder connections were positively affected by time, which suggests the degrade of local density and upgrade of feeder density ratio could help brain get a new communication balance.

Plausible neuroarchitectural underpinning of poststroke functions and functional recovery

Investigation of the neuroarchitectural underpinning of functions of stroke patients showed that the network properties that were correlated to functional assessments were not related to structural connections to/from rich-club regions, except the mean length of feeder connection. Local connections reflect feeder and rich club connections together since they form all connections of the whole network together. the communication cost ratio of local connections decreases will give more communication cost ratio of feeder and rich club connections, which support functions of brain network more, so that the UE-FM score and BI may be higher. Decreased mean length of feeder and local connections may help reduce the communication time between a rich club region and a local region as well as a local region and another local region as functionally recovered.

For the neuroarchitectural underpinning of poststroke functional recovery (change in functional assessment from baseline), our results showed that improvement in BI was correlated with higher communication cost ratio of feeder connections, lower density, lower communication cost ratio of local connections, and that improvement in UE-FM was correlated with lower communication cost of rich-club connections, lower cost, lower communication cost, higher communication cost ratio of feeder connections, lower density , lower length, lower cost, lower communication cost and lower communication cost ratio of local connections.

However, the rich club changes present in the normalized rich club coefficients, a range of normalized rich club coefficients were significantly correlated with UE-FM (k=20) and BI ($17 \leq k \leq 22$) scores respectively as has been observed in patients with Alzheimer's disease[27]. The reason of this phenomenon may be increased rich club coefficient causes increased capacity of the rich club organization so that it can serve brain motor function better.

It is noteworthy that of all the metrics of brain network at rich-club scale that correlate with poststroke functional recovery, density of local connections, communication cost of rich-club connections, communication cost ratio of feeder connections, and normalized rich-club coefficient could potentially be prognostic indicators of stroke recovery. Our findings extended the work by Ktena et al [29] and Schirmer et al [28] in modelling poststroke functional outcome. Both of their work demonstrated that the prediction of stroke functional outcome could be improved by the incorporation of the number of rich club regions that were affected by stroke.

Limitations

Our study still has several limitations. First, the infarct was located in different hemispheres among the 16 patients. To avoid systematic error, we swapped the brain regions from the two hemispheres for patients with right-sided infarct to ensure that all infarcts were on the left hemisphere. However, brain asymmetry may have confounded our results; for example, the strengths of the left and right hemispheres are not equal [45]. Second, there were some missing data in our dataset due to patient attrition. We have nonetheless partially circumvented this problem using data imputation. Finally, we did not have data from control group in order to investigate the effect of stroke on rich-club organizations.

References

(1) Langhorne, P.; Coupar, F.; Pollock, A. Motor Recovery after Stroke: A Systematic Review. *The Lancet Neurology* **2009**, *8* (8), 741–754.

(2) Warlow, C. P.; Van Gijn, J.; Dennis, M. S.; Wardlaw, J. M.; Bamford, J. M.; Hankey, G. J.; Sandercock, P. A.; Rinkel, G.; Langhorne, P.; Sudlow, C. *Stroke: Practical Management*; John Wiley & Sons, 2011.

(3) Johansson, B. B. Brain Plasticity and Stroke Rehabilitation: The Willis Lecture. *Stroke* **2000**, *31* (1), 223–230.

(4) Murphy, T. H.; Corbett, D. Plasticity during Stroke Recovery: From Synapse to Behaviour. *Nature Reviews Neuroscience* **2009**, *10* (12), 861–872.

(5) Schaechter, J. D. Motor Rehabilitation and Brain Plasticity after Hemiparetic Stroke. *Progress in neurobiology* **2004**, *73* (1), 61–72.

(6) Di Pino, G.; Pellegrino, G.; Assenza, G.; Capone, F.; Ferreri, F.; Formica, D.; Ranieri, F.; Tombini, M.; Ziemann, U.; Rothwell, J. C. Modulation of Brain Plasticity in Stroke: A Novel Model for Neurorehabilitation. *Nature Reviews Neurology* **2014**, *10* (10), 597–608.

(7) Ward, N. S.; Newton, J. M.; Swayne, O. B.; Lee, L.; Thompson, A. J.; Greenwood, R. J.; Rothwell, J. C.; Frackowiak, R. S. Motor System Activation after Subcortical Stroke Depends on Corticospinal System Integrity. *Brain* **2006**, *129* (3), 809–819.

(8) Kirton, A.; Shroff, M.; Visvanathan, T.; Deveber, G. Quantified Corticospinal Tract Diffusion Restriction Predicts Neonatal Stroke Outcome. *Stroke* **2007**, *38* (3), 974–980.

(9) Stinear, C. M.; Barber, P. A.; Smale, P. R.; Coxon, J. P.; Fleming, M. K.; Byblow, W. D. Functional Potential in Chronic Stroke Patients Depends on Corticospinal Tract Integrity. *Brain* **2007**, *130* (1), 170–180.

(10) Zhu, L. L.; Lindenberg, R.; Alexander, M. P.; Schlaug, G. Lesion Load of the Corticospinal Tract Predicts Motor Impairment in Chronic Stroke. *Stroke* **2010**, *41* (5), 910–915.

(11) Newton, J. M.; Ward, N. S.; Parker, G. J.; Deichmann, R.; Alexander, D. C.; Friston, K. J.; Frackowiak, R. S. Non-Invasive Mapping of Corticofugal Fibres from Multiple Motor Areas—Relevance to Stroke Recovery. *Brain* **2006**, *129* (7), 1844–1858.

(12) Lindberg, P. G.; Skejø, P. H.; Rounis, E.; Nagy, Z.; Schmitz, C.; Wernegren, H.; Bring, A.; Engardt, M.; Forssberg, H.; Borg, J. Wallerian Degeneration of the Corticofugal Tracts in Chronic Stroke: A Pilot Study Relating Diffusion Tensor Imaging, Transcranial Magnetic Stimulation, and Hand Function. *Neurorehabilitation and neural repair* **2007**, *21* (6), 551–560.

(13) Strens, L. H. A.; Asselman, P.; Pogosyan, A.; Loukas, C.; Thompson, A. J.; Brown, P. Corticocortical Coupling in Chronic Stroke: Its Relevance to Recovery. *Neurology* **2004**, *63* (3), 475–484.

(14) Feydy, A.; Carlier, R.; Roby-Brami, A.; Bussel, B.; Cazalis, F.; Pierot, L.; Burnod, Y.; Maier, M. A. Longitudinal Study of Motor Recovery after Stroke: Recruitment and Focusing of Brain Activation. *Stroke* **2002**, *33* (6), 1610–1617.

(15) Schulz, R.; Braass, H.; Liuzzi, G.; Hoerniss, V.; Lechner, P.; Gerloff, C.; Hummel, F. C. White Matter Integrity of Premotor–Motor Connections Is Associated with Motor Output in Chronic Stroke Patients. *NeuroImage: Clinical* **2015**, *7*, 82–86.

(16) Crofts, J. J.; Higham, D. J.; Bosnell, R.; Jbabdi, S.; Matthews, P. M.; Behrens, T. E. J.; Johansen-Berg, H. Network Analysis Detects Changes in the Contralesional Hemisphere Following Stroke. *Neuroimage* **2011**, *54* (1), 161–169.

(17) Colizza, V.; Flammini, A.; Serrano, M. A.; Vespignani, A. Detecting Rich-Club Ordering in Complex Networks. *Nature physics* **2006**, *2* (2), 110.

(18) McAuley, J. J.; da Fontoura Costa, L.; Caetano, T. S. Rich-Club Phenomenon across Complex Network Hierarchies. *Applied Physics Letters* **2007**, *91* (8), 084103.
(19) Harriger, L.; Van Den Heuvel, M. P.; Sporns, O. Rich Club Organization of Macaque Cerebral Cortex and Its Role in Network Communication. *PloS one* **2012**, *7* (9), e46497.
(20) van den Heuvel, M. P.; Kahn, R. S.; Goñi, J.; Sporns, O. High-Cost, High-Capacity Backbone for Global Brain Communication. *Proceedings of the National Academy of Sciences* **2012**, *109* (28), 11372–11377.
(21) Senden, M.; Deco, G.; de Reus, M. A.; Goebel, R.; van den Heuvel, M. P. Rich Club Organization Supports a Diverse Set of Functional Network Configurations. *Neuroimage* **2014**, *96*, 174–182.
(22) Van Den Heuvel, M. P.; Sporns, O. Rich-Club Organization of the Human Connectome. *Journal of Neuroscience* **2011**, *31* (44), 15775–15786.
(23) van den Heuvel, M. P.; Sporns, O.; Collin, G.; Scheewe, T.; Mandl, R. C.; Cahn, W.; Goñi, J.; Pol, H. E. H.; Kahn, R. S. Abnormal Rich Club Organization and Functional Brain Dynamics in Schizophrenia. *JAMA psychiatry* **2013**, *70* (8), 783–792.
(24) McColgan, P.; Seunarine, K. K.; Razi, A.; Cole, J. H.; Gregory, S.; Durr, A.; Roos, R. A.; Stout, J. C.; Landwehrmeyer, B.; Scahill, R. I. Selective Vulnerability of Rich Club Brain Regions Is an Organizational Principle of Structural Connectivity Loss in Huntington's Disease. *Brain* **2015**, *138* (11), 3327–3344.
(25) Shu, N.; Duan, Y.; Huang, J.; Ren, Z.; Liu, Z.; Dong, H.; Barkhof, F.; Li, K.; Liu, Y. Progressive Brain Rich-Club Network Disruption from Clinically Isolated Syndrome towards Multiple Sclerosis. *NeuroImage: Clinical* **2018**, *19*, 232–239.
(26) Verhelst, H.; Vander Linden, C.; De Pauw, T.; Vingerhoets, G.; Caeyenberghs, K. Impaired Rich Club and Increased Local Connectivity in Children with Traumatic Brain Injury: Local Support for the Rich? *Human brain mapping* **2018**, *39* (7), 2800–2811.
(27) Yan, T.; Wang, W.; Yang, L.; Chen, K.; Chen, R.; Han, Y. Rich Club Disturbances of the Human Connectome from Subjective Cognitive Decline to Alzheimer's Disease. *Theranostics* **2018**, *8* (12), 3237.
(28) Schirmer, M. D.; Ktena, S. I.; Nardin, M. J.; Donahue, K. L.; Giese, A.-K.; Etherton, M.; Wu, O.; Rost, N. Rich-Club Organization: An Important Determinant of Functional Outcome after Acute Ischemic Stroke. *Frontiers in neurology* **2019**, *10*, 956.
(29) Ktena, S. I.; Schirmer, M. D.; Etherton, M. R.; Giese, A.-K.; Tuozzo, C.; Mills, B. B.; Rueckert, D.; Wu, O.; Rost, N. S. Brain Connectivity Measures Improve Modeling of Functional Outcome after Acute Ischemic Stroke. *Stroke* **2019**, *50* (10), 2761–2767.
(30) Sullivan, K. J.; Tilson, J. K.; Cen, S. Y.; Rose, D. K.; Hershberg, J.; Correa, A.; Gallichio, J.; McLeod, M.; Moore, C.; Wu, S. S. Fugl-Meyer Assessment of Sensorimotor Function after Stroke: Standardized Training Procedure for Clinical Practice and Clinical Trials. *Stroke* **2011**, *42* (2), 427–432.
(31) Kwakkel, G.; Veerbeek, J. M.; Harmeling-van der Wel, B. C.; van Wegen, E.; Kollen, B. J. Diagnostic Accuracy of the Barthel Index for Measuring Activities of Daily Living Outcome after Ischemic Hemispheric Stroke: Does Early Poststroke Timing of Assessment Matter? *Stroke* **2011**, *42* (2), 342–346.
(32) Andersson, J. L.; Skare, S. A Model-Based Method for Retrospective Correction of Geometric Distortions in Diffusion-Weighted EPI. *Neuroimage* **2002**, *16* (1), 177–199.
(33) Talairach, J. 3-Dimensional Proportional System; an Approach to Cerebral Imaging. Co-Planar Stereotaxic Atlas of the Human Brain. *Thieme* **1988**, 1–122.

(34) Wang, R.; Benner, T.; Sorensen, A. G.; Wedeen, V. J. Diffusion Toolkit: A Software Package for Diffusion Imaging Data Processing and Tractography. In *Proc Intl Soc Mag Reson Med*; Berlin, 2007; Vol. 15.
(35) Mori, S.; Crain, B. J.; Chacko, V. P.; Van Zijl, P. C. Three-Dimensional Tracking of Axonal Projections in the Brain by Magnetic Resonance Imaging. *Annals of Neurology: Official Journal of the American Neurological Association and the Child Neurology Society* **1999**, *45* (2), 265–269.
(36) Mori, S.; Van Zijl, P. C. Fiber Tracking: Principles and Strategies–a Technical Review. *NMR in Biomedicine: An International Journal Devoted to the Development and Application of Magnetic Resonance In Vivo* **2002**, *15* (7–8), 468–480.
(37) Rolls, E. T.; Joliot, M.; Tzourio-Mazoyer, N. Implementation of a New Parcellation of the Orbitofrontal Cortex in the Automated Anatomical Labeling Atlas. *Neuroimage* **2015**, *122*, 1–5.
(38) Opsahl, T.; Colizza, V.; Panzarasa, P.; Ramasco, J. J. Prominence and Control: The Weighted Rich-Club Effect. *Physical review letters* **2008**, *101* (16), 168702.
(39) Ball, G.; Aljabar, P.; Zebari, S.; Tusor, N.; Arichi, T.; Merchant, N.; Robinson, E. C.; Ogundipe, E.; Rueckert, D.; Edwards, A. D. Rich-Club Organization of the Newborn Human Brain. *Proceedings of the National Academy of Sciences* **2014**, *111* (20), 7456–7461.
(40) Bullmore, E.; Vértes, P. From Lichtheim to Rich Club: Brain Networks and Psychiatry. *JAMA psychiatry* **2013**, *70* (8), 780–782.
(41) van den Heuvel, M. P.; Kahn, R. S.; Goñi, J.; Sporns, O. High-Cost, High-Capacity Backbone for Global Brain Communication. *Proceedings of the National Academy of Sciences* **2012**, *109* (28), 11372–11377.
(42) Cnaan, A.; Laird, N. M.; Slasor, P. Using the General Linear Mixed Model to Analyse Unbalanced Repeated Measures and Longitudinal Data. *Statistics in medicine* **1997**, *16* (20), 2349–2380.
(43) Verbeke, G.; Molenberghs, G. *Linear Mixed Models for Longitudinal Data*; Springer Science & Business Media, 2009.
(44) Winter, B. Linear Models and Linear Mixed Effects Models in R with Linguistic Applications. *arXiv preprint arXiv:1308.5499* **2013**.
(45) de Reus, M. A.; van den Heuvel, M. P. Rich Club Organization and Intermodule Communication in the Cat Connectome. *Journal of Neuroscience* **2013**, *33* (32), 12929–12939.
(46) Murphy, T. H.; Corbett, D. Plasticity during Stroke Recovery: From Synapse to Behaviour. *Nature Reviews Neuroscience* **2009**, *10* (12), 861.
(47) McColgan, P.; Seunarine, K. K.; Razi, A.; Cole, J. H.; Gregory, S.; Durr, A.; Roos, R. A.; Stout, J. C.; Landwehrmeyer, B.; Scahill, R. I. Selective Vulnerability of Rich Club Brain Regions Is an Organizational Principle of Structural Connectivity Loss in Huntington's Disease. *Brain* **2015**, *138* (11), 3327–3344.
(48) Van Den Heuvel, M. P.; Sporns, O. Rich-Club Organization of the Human Connectome. *Journal of Neuroscience* **2011**, *31* (44), 15775–15786.